Materials Letters 179 (2016) 118–121

Contents lists available at ScienceDirect

Materials Letters

journal homepage: www.elsevier.com/locate/matlet

Tribocorrosion behavior of β-type Ti-15Zr-based alloys

D.R.N. Correa [a,b,*], P.A.B. Kuroda [a,b], C.R. Grandini [a,b], L.A. Rocha [a,b,c], F.G.M. Oliveira [b,c], A.C. Alves [c], F. Toptan [b,d]

[a] UNESP – Univ Estadual Paulista, Laboratório de Anelasticidade e Biomateriais, Bauru, SP, Brazil
[b] UNESP Univ Estadual Paulista, IBTN/Br, Instituto de Biomateriais, Tribocorrosão e Nanomedicina, Bauru, SP, Brazil
[c] CMEMS-UMinho – Center of MicroElectroMechanical Systems, Guimarães, Portugal
[d] University of Minho – DEM – Department of Mechanical Engineering – Guimarães, Portugal

ARTICLE INFO

Article history:
Received 16 December 2015
Received in revised form
30 March 2016
Accepted 7 May 2016
Available online 10 May 2016

Keywords:
Titanium alloys
Mechanical properties
Tribocorrosion
Biomaterial

ABSTRACT

Titanium alloys have different biomedical applications, due to their favorable mechanical, electrochemical and biological properties. However, when applied as orthopedical or dental implants, the metallic material is submitted to intense mechanical wear in a corrosive environment. In general, tribocorrosion behavior is disregarded during the development of new titanium alloys, which is focused on better mechanical or biological compatibility. In this paper, the tribocorrosion behavior of novel titanium alloys, Ti-15Zr-7.5Mo and Ti-15Zr-15Mo, for biomedical applications was investigated. Tribocorrosion tests were performed against an alumina sphere, with OCP and COF monitored during sliding. Average total wear volume was calculated by tridimensional images with confocal microscopy. The results indicated that both alloys present tribocorrosion behavior superior to cp-Ti, being abrasion the main wear mechanism. Wear volume analysis showed that the Ti-15Zr-7.5Mo presented the better tribocorrosion properties, besides the higher Young's modulus.

1. INTRODUCTION

Titanium and its alloys have biomedical applications, mainly in orthopedic and dental implants [1,2] due to their well-known properties as high specific strength, low Young's modulus, excellent corrosion resistance, good biocompatibility and osseointegration [1,3].

New Ti-based alloys have been developed with Al- and V-free materials, due the adverse reactions those elements may have with tissue and cells [3,4]. The main alloying elements chosen are Mo, Zr, Nb and Ta, which are considered as non-cytotoxic metals. Furthermore, β-type Ti-based alloys exhibit Young's modulus, closer to hard tissues, avoiding stress shielding effect [2,3,5].

For orthopedic and dental implants, tribocorrosion resistance is an important factor to consider, because the concurrent action of wear and corrosion may lead to accelerated degradation of the implant [6,7]. Hip-joint stems and dental implants can suffer wear by friction of the material with bone, due to the inherent loading conditions. This process happens in a corrosive environment that can produce surface damage, committing osseointegration and facilitating bacterial activity [8].

Titanium shows the ability to form a stable oxide layer that ensures protection, good corrosion resistance and biocompatibility. However, the passive layer has low wear resistance, and can be removed by mechanical stresses [9]. In the oral zone, successive micro-movements between the interface bone-implant can result in the liberation of particles, which have potential harmful effects [10].

Bio-tribocorrosion of biomedical Ti alloys was the focus of recent studies, although there is still relatively low knowledge of the wear and corrosion mechanisms occurring at the metallic surface [11,12]. This work aims to report, for the first time, the tribocorrosion properties of Ti-15Zr-based alloys with β stable and metastable structures.

2. Materials and methods

The alloys were produced by argon arc-melting with commercially pure metals, being remelted for 5 times. The ingots were submitted to hot-rolling (1000 °C), with air cooling. After that, were carried out a homogenization treatment, at 1000 °C, during 24 h, followed by slow cooling. The chemical composition was analyzed by ICP-OES, thermo-conductivity and infrared optical absorption. Density was measured by Archimedes' principle. Selected area diffraction (SAD) was obtained in a TEM Titan

* Corresponding author at: UNESP - Univ Estadual Paulista, Laboratório de Anelasticidade e Biomateriais, Bauru, SP, Brazil.

http://dx.doi.org/10.1016/j.matlet.2016.05.045
0167-577X/

Table 1
Chemical, physical, microstructural and mechanical characteristics.

	Ti-15Zr-7.5Mo	Ti-15Zr-15Mo
Ti (wt%)	Balance	Balance
Zr (wt%)	14.75	14.80
Mo (wt%)	7.36	14.25
Others (wt%)	< 1	< 1
O (wt%)	0.14	0.34
N (wt%)	0.04	0.04
Density (g/cm^3)	4.99 ± 0.02	5.25 ± 0.01
Structure	β+α″+(ω)	β
Microstructure	Grains with acicular structures	Equiaxed grains
Vickers hardness (HV)	479 ± 3	398 ± 3
Young's modulus (GPa)	114 ± 5	74 ± 4

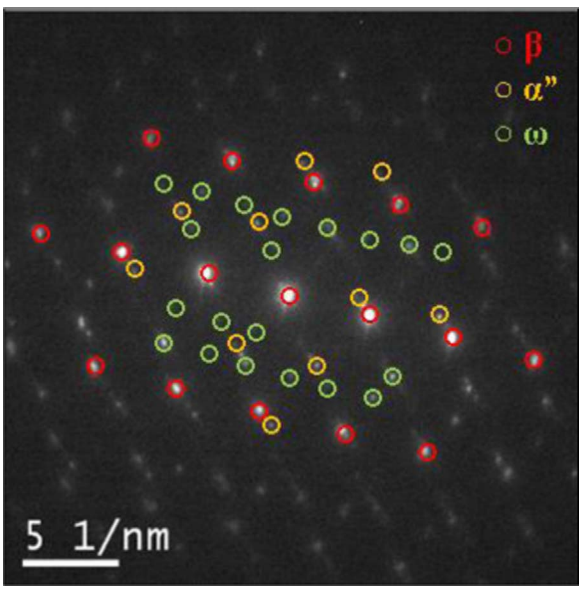

Fig. 1. SAD of the Ti-15Zr-7.5Mo alloy.

equipment, operating at 300 kV. Vickers microhardness was carried out in Shimadzu HMV-2 equipment, with 0.200 kgf (1.961 N), for 60 s Young's modulus was obtained by excitation impulse method in a Sonelastic's equipment.

The tribocorrosion tests were carried out in three polished square samples, with area around 1 cm^2, in SBF solution at 37 °C [13]. The tests were carried out in a tribometer CETR-UMT2, pin-on-disk configuration, with alternative sliding. The three electrodes configuration were utilized, with the samples as work electrode, saturated calomel (Hg/Hg_2Cl_2/saturated KCl solution) as reference electrode, and platinum as auxiliary electrode. Alumina spheres (10 mm diameter) was used as counter body, being the sliding performed with 5 mm of amplitude, at 2 Hz and load of 1.5 N, during 30 min. Electrochemical measurements were carried out in a potentiostat Radiometer Copenhagen (PGP201), being the samples immersed in the solution 1 h before the sliding, for potential stabilization. The open circuit potential (OCP) and coefficient of friction (COF) was evaluated along the test. The wear track was analyzed by SEM (EVO LS15, Carl Zeiss) and confocal optical microscopy (DCM3D, Leica).

3. Results and discussion

Table 1 presents the specific properties of the alloys after heat treatment. The chemical composition remained within values closed to the nominal composition. Also, metallic impurities are

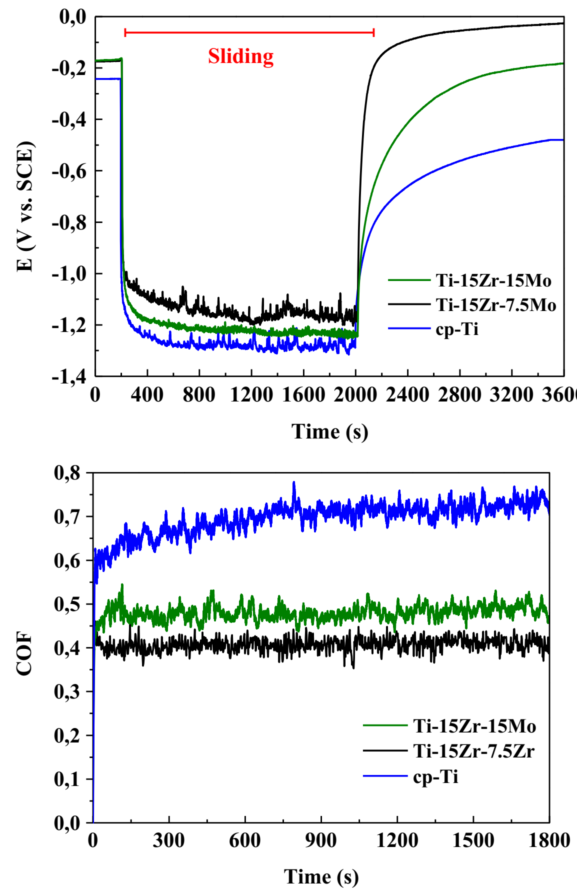

Fig. 2. Tribocorrosion results.

present in low concentration, while interstitial elements (oxygen and nitrogen) show adequate values. Density remained higher than cp-Ti (4.51 ± 0.02 g/cm^3), due the higher density of the Zr (6.51 g/cm^3) and Mo (10.22 g/cm^3). Ti-15Zr-7.5Mo exhibited a biphasic structure α″+β, in the form of fine needles around the β grains, while Ti-15Zr-15Mo showed only equiaxial grains of β phase. The heat treated microstructure tended to originate phases near to the equilibrium, due the slow cooling from the β field, being dependent on the alloy composition. Reports on the Ti-Mo system have suggested the possible precipitation of the metastable ω phase for intermediary concentrations of β-stabilizers, which could results in high hardness and embrittlement effect [1,14]. Regarding mechanical properties, the hardness and Young's modulus were dependent of the composition and microstructure (see Table 1). Hardness of both alloys was higher than cp-Ti (187 ± 5 HV), due mechanisms of solid solution and phase precipitation hardening [5,15]. Young's modulus of the Ti-15Zr-7.5Mo shows values slightly higher than cp-Ti (105 ± 2 GPa). Together with the high values of hardness, ω phase precipitation might have occurred [1,16]. It was confirmed by SAD analysis, where were observed diffraction points of ω phase (Fig. 1). However, the β-type Ti-15Zr-15Mo presented lower Young's modulus, due the bcc structure [4], being, from this point of view, more interesting for application in osseointegrated implants.

In Fig. 2, the evolution of the OCP during the tribocorrosion tests is presented. Before the sliding, OCP of both alloys were similar, indicating identical tendency to corrosion. Before starting of the sliding, OCP of cp-Ti is slightly lower than the alloys, indicating a higher reactivity. When sliding starts, all samples showed an abrupt fall of the potential, which is usually attributed to the destruction of the passive layer [6]. Potential values stabilized

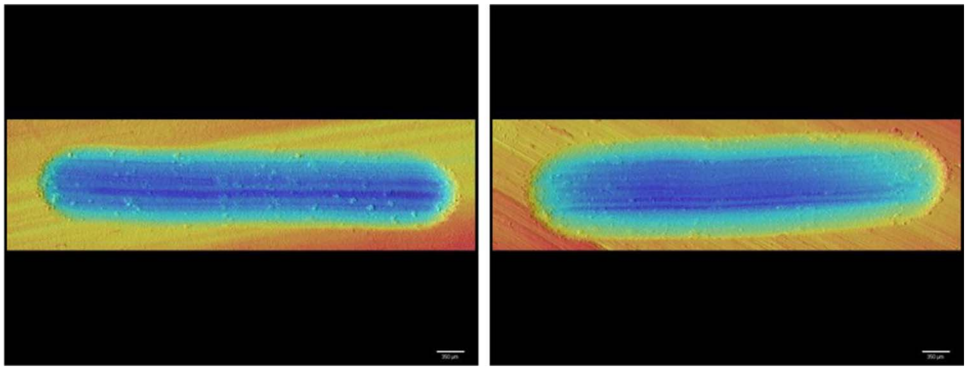

Fig. 3. Confocal micrographs: Ti-15Zr-7.5Mo (left) and Ti-15Zr-15Mo (right).

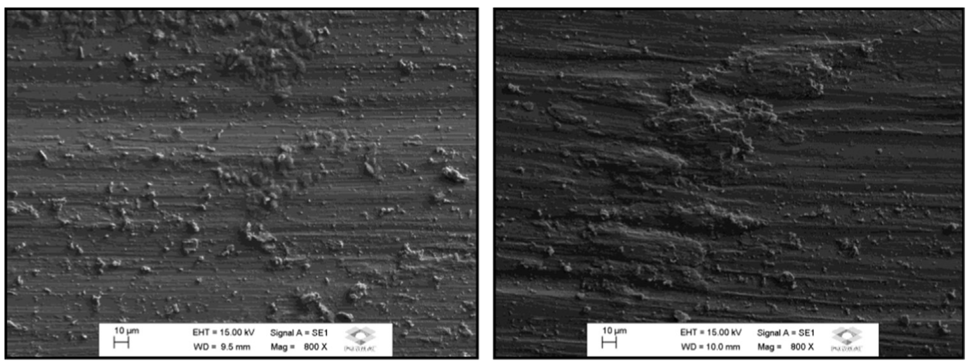

Fig. 4. SEM images: Ti-15Zr-7.5Mo (left) and Ti-15Zr-15Mo (right).

slightly above the cp-Ti, between −1.1 V and −1.2 V, with small oscillations during the sliding. The potential oscillations were related with the phenomena of destruction and recovery of the passive layer during the process [17]. About COF evolution (Fig. 2), it was possible to observe slightly higher values for Ti-15Zr-15Mo ($\mu \approx 0.5$) when compared to Ti-15Zr-7.5Mo ($\mu \approx 0.4$). When the mechanical contact is stopped, repassivation occurs in all samples [18]. Repassivation of the passive layer, means that a new barrier against corrosion is formed on the surface [7]. In the end, Ti-15Zr-7.5Mo had a higher potential value than before the sliding, indicating a great recovery capacity of the oxide layer [17,19].

In the Fig. 3, wear track images, obtained by confocal microscopy, are shown. There was a regular wear track in both alloys, having the Ti-15Zr-7.5Mo a smaller width, corresponding to a lower wear volume. The average wear volume of the alloys remained around 224 ± 9 mm^3 and 281 ± 13 mm^3 for Ti-15Zr-7.5Mo and Ti-15Zr-15Mo, respectively. Ti-15Zr-7.5Mo showed a lower quantity of wear volume, being related with the high hardness (high mechanical strength) [4]. A low wear volume is important for biomaterials, in order to minimize metallic ions liberation which can induce adverse reactions in the body [3,20]. Although Ti-15Zr-7.5Mo do not present most favorable elastic modulus for biomedical applications, its tribocorrosion properties are very interesting for use in corrosive and wear environment.

In the Fig. 4 are presented SEM images of the wear track. Ti-15Zr-7.5Mo showed abrasion grooves and small dark points, indicating a possible plastic deformation of the acicular structures [11]. Ti-15Zr-15Mo presented only wear grooves in the sliding direction, indicating only an abrasion mechanism [11,17]. The alloys have had the same wear abrasion mechanism, although Ti-15Zr-15Mo showed more abrasion areas [17]. Lee et al. [21] observed similar plastic deformation in TNTZ alloys and Ti-6Al-4 V when submitted to wear tests.

4. Conclusions

Ti-15Zr-based alloys with two molybdenum content were prepared and compared by your mechanical and tribocorrosion properties. Microstructures were composed by equiaxial grains (β phase) and acicular structures (α'' phase). Hardness and Young's modulus of the Ti-15Zr-7.5Mo presented evidences of ω phase, considered harmful in the biomedical area, while Ti-15Zr-15Mo presented a better mechanical compatibility, with high hardness and low Young's modulus.

Tribocorrosion tests indicated similar corrosion potential and wear mechanisms of the alloys, having showed corrosion and wear resistance, and passivation capacity better than cp-Ti. Ti-15Zr-7.5Mo had a low wear volume, indicating a better behavior in a corrosive environment. Furthermore, Ti-15Zr-7.5Mo could have potential for dental applications, where the resistance of corrosive and abrasive environment is more important factor than mechanical properties.

Acknowledgements

The authors acknowledge the Marília Afonso Rabelo Buzalaf and Paulo Noronha Lisboa Filho by the collaboration, INMETRO by the TEM and SAD analysis, and Brazilian agencies CNPq (#481313/2012-5 and #307.279/2013-8) and FAPESP (#2010/20.440-7) for their financial support.

References

[1] D. Banerjee, J.C. Williams, Acta Mater. 61 (2013) 844.
[2] Y. Li, C. Yang, H. Zhao, S. Qu, X. Li, Y. Li, Materials 7 (2014) 1709.
[3] M. Geetha, A.K. Singh, R. Asokamani, A.K. Gogia, Prog. Mater. Sci. 54 (2009) 397.
[4] M. Niinomi, M. Nakai, J. Hieda, Acta Biomater. 8 (2012) 3888.

[5] D.R.N. Correa, P.A.B. Kuroda, C.R. Grandini, Adv. Mater. Res. 922 (2014) 75.
[6] S. Mischler, Tribol. Int. 41 (2008) 573.
[7] P. Ponthiaux, F. Wenger, D. Drees, J.P. Celis, Wear 256 (2004) 459.
[8] P. Senna, A. Antoninha Del Bel Cury, S. Kates, L. Meirelles, Clin. Implant Dent. Relat. Res. (2013).
[9] N. Diomidis, J.P. Celis, P. Ponthiaux, F. Wenger, Lubr. Sci. 21 (2009) 53.
[10] N.J. Hallab, J.J. Jacobs, Bull. NYU Hosp. Jt. Dis. 67 (2009) 182.
[11] M.J. Runa, M.T. Mathew, L.A. Rocha, Tribol. Int. 68 (2013) 85.
[12] N.S. More, N. Diomidis, S.N. Paul, M. Roy, S. Mischler, Mater. Sci. Eng.: C 31 (2011) 400.
[13] M. Bohner, J. Lemaitre, Biomaterials 30 (2009) 2175.
[14] E. Sukedai, M. Shimoda, H. Nishizawa, Y. Nako, Mater. Trans. 52 (2011) 324.
[15] D.R. Correa, F.B. Vicente, T.A. Donato, V.E. Arana-Chavez, M.A. Buzalaf, C. R. Grandini, Mater. Sci. Eng.: C 34 (2014) 354.
[16] X. Zhao, M. Niinomi, M. Nakai, J. Hieda, Acta Biomater. 8 (2012) 1990.
[17] A.C. Alves, F. Oliveira, F. Wenger, P. Ponthiaux, J.P. Celis, L.A. Rocha, J. Phys. D: Appl. Phys. 46 (2013) 404001.
[18] T. Hanawa, K. Asami, K. Asaoka, J. Biomed. Mater. Res. 40 (1998) 530.
[19] N.T.C. Oliveira, A.C. Guastaldi, Corros. Sci. 50 (2008) 938.
[20] M. Abdel-Hady Gepreel, M. Niinomi, J. Mech. Behav. Biomed. Mater. 20 (2013) 407.
[21] Y.S. Lee, M. Niinomi, M. Nakai, K. Narita, K. Cho, J. Mech. Behav. Biomed. Mater. 41 (2015) 208.